Aquaculture 579 (2024) 740200

Contents lists available at ScienceDirect

Aquaculture

journal homepage: www.elsevier.com/locate/aquaculture

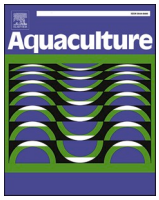

Integration of transcriptome and metabolome reveals molecular mechanisms responsive to cold stress in gynogenetic mrigal carp (*Cirrhinus mrigala*)

Hongqing Li [a,1], Wuhui Li [b,c,1], Jisen Su [a,1], Zexun Zhou [c], Yan Miao [c], Xuelei Tian [d], Min Tao [b,c], Chun Zhang [b,c], Yi Zhou [b,c], Qinbo Qin [b,c], Huirong Yang [a,e,*], Shaojun Liu [a,b,c,*]

[a] College of Marine Sciences, South China Agricultural University, Guangzhou 510642, China
[b] Guangdong Laboratory for Lingnan Modern Agriculture, Guangzhou 510642, China
[c] State Key Laboratory of Developmental Biology of Freshwater Fish, College of Life Sciences, Hunan Normal University, Changsha 410081, China
[d] Guangzhou Chengyi Aquaculture Co., Ltd, Guangzhou 510642, China
[e] Zhongshan Innovation Center of South China Agricultural University, Zhongshan 528400, China

ARTICLE INFO

Keywords:
Gynogenetic mrigal carp
Cold stress
Transcriptomes
Metabolomics
Pathways

ABSTRACT

Cold stress is a major environmental stimulus affecting the physiological and metabolic activities of farmed fish. In our previous study, we obtained gynogenetic mrigal carp (*Cirrhinus mrigala*, GMC) with significantly improved cold tolerance compared with the wild individuals. To gain a comprehensive and unbiased understanding of the molecular mechanism of cold tolerance in GMC, transcriptomes and metabolomics of liver tissues were comparatively analysed. After cold treatment at 14 °C for 48 h, histology analysis revealed that the hepatocyte nucleus was shifted, blurred and disintegrated; the terminus of the gill filament was enlarged; and the number of mucus cells and their secretions were increased. A total of 4844 differentially expressed genes (DEGs), including 2420 upregulated and 2424 downregulated genes, were identified. The upregulated KEGG pathways were mainly involved in oxidative phosphorylation, the proteasome and the citrate cycle, while the downregulated pathways were involved in staphylococcus aureus infection, systemic lupus erythematosus and leishmaniasis. A total of 160 differential metabolites (DMs) were identified, including 39 increased and 121 reduced metabolites. The KEGG pathway analysis revealed significant enrichment in retinol metabolism and folate biosynthesis. KEGG function analysis showed that the DEGs and DMs were both highly enriched in purine metabolism, neuroactive ligand–receptor interaction and galactose metabolism. Correlation analysis between DEGs and DMs revealed that multiple pathways were active and strongly related to immunity and disease, metabolism and growth under cold stress. This study can facilitate our understanding of the molecular mechanisms of fish response to cold stress and provide insight into the application of gynogenesis in farmed fish.

1. Introduction

Water temperature is a crucial environmental factor that profoundly influences aquatic organisms' life activities, including their survival, growth, behavioural and physiological responses (Islam et al., 2022; Little et al., 2020). As ectotherms, fishes can cape with natural temperature changes within species-specific thermal tolerance ranges. However, when the temperature changes below the tolerance capability of fish, cold stress activates a cascade of events that may lead to loss of balance and even coma, ultimately leading to death (Panase et al., 2018). For instance, tilapia (*Oreochromis niloticus*) and mrigal carp (*Cirrhinus mrigala*, MC) are not able to survive at water temperatures lower than 10 °C (Atwood et al., 2003; Yu et al., 2019). It has been shown that some cold-water fish species have evolved adaptive mechanisms, including transcriptomic and genomic evolution to cope with cold stress to protect them against damage (Chen et al., 2008). Meanwhile, several fish species, such as goldfish (*Carassius auratus*) and zebrafish (*Danio rerio*), survive and adapt to cold stress by remodeling the structure of their gills and heart (Johnson et al., 2014; Mitrovic and Perry, 2009).

* Corresponding authors at: College of Marine Sciences, South China Agricultural University, Guangzhou 510642, China.
E-mail addresses: hry@scau.edu.cn (H. Yang), lsj@hunnu.edu.cn (S. Liu).
[1] These authors have contributed equally to this work.

https://doi.org/10.1016/j.aquaculture.2023.740200
Received 26 April 2023; Received in revised form 18 August 2023; Accepted 7 October 2023
Available online 9 October 2023

The effects of cold stress on fish individuals and cells have been well documented in recent decades. Acute or chronic exposure to low temperatures can slow the rate of fish growth, impair the immunity and disease defense ability and compromise the overall health of fish (Abram et al., 2017; Yang et al., 2016). The liver is a significant organ for fish to adapt to temperature changes; many studies have reported that cold stress has caused hepatocyte degeneration, metabolic disorders, DNA damage, and altered liver gene expression (Reid et al., 2022; Sun et al., 2019a). The gills of fish are sensitive to environmental changes and exhibit significant morphological plasticity in response to temperature changes (Wen et al., 2018). To gain a comprehensive understanding of the changes in the organisms, transcriptomics and metabolomics have been widely used to investigate the molecular mechanism of cold stress. For example, in tiger barb (*Puntius tetrazona*) (Liu et al., 2020), common carp (*Cyprinus carpio*) (Ge et al., 2020), tilapia (*Oreochromis niloticus*) (Nitzan et al., 2019) and taimen (*Hucho taimen*) (Liu et al., 2021), transcriptomics analysis revealed that changes in global gene expression were associated with energy metabolism, immune functions, oxidative damage and cell apoptosis. Metabolomics analysis revealed that cold stress has different effects on energy metabolism, methionine cycling, glutathione metabolism, lipid catabolism and antioxidant defense in different tissues (Ghisaura et al., 2019; Schleger et al., 2022; Wen et al., 2019). In addition, multi omics analysis was developed to explore the regulatory mechanisms between gene expression and metabolites (Jiang et al., 2023; Liu et al., 2022; Wen et al., 2019). There have been several studies of cold resistance in fish. However, the knowledge regarding the mechanisms underlying fish responses to cold stress, precisely how and to what extent organisms adapt to cold stress at various molecular and physiological levels, still needs to be improved.

Artificial gynogenesis, an induced developmental process in which the maternal genome is activated by genetically inactivated sperm, is an important method to accelerate the selective breeding of varieties and populations (Manan et al., 2022; Xu et al., 2015). In many farmed fishes, artificial gynogenetic offspring have been reported to exhibit superior traits such as fast growth rates, hypoxia tolerance and strong resistance to diseases (Li et al., 2015; Wu et al., 2021; Xiao et al., 2011). Nevertheless, the molecular mechanisms of those superior traits in artificial gynogenetic fish have yet to be well studied. In our previous study, gynogenetic mrigal carp (GMC, 2n = 50) was successfully established, and this population showed a higher cold tolerance for surviving over winter at temperatures below 10 °C. Moreover, lower critical thermal minimum (CTMin) and lethal temperature (T_{LD50}) values were detected in GMC than in MC fish (Li et al., 2023). Herein, to gain a comprehensive and unbiased molecular understanding of cold tolerance in GMC, GMC fish were firstly cooled from 26 °C to 14 °C at 36 h and then treated at 14 °C for 48 h, the transcriptomes and metabolomics of liver tissues were comparatively analysed between GMC and MC fish. The results of this study can facilitate our understanding of the molecular mechanisms of fish responses to cold stress and provide insight into the application of gynogenetic methods to farmed fish.

2. Materials and methods

2.1. Ethics approval and consent to participate

Animal experimenters were certified via a professional training course for laboratory animal practitioners by South China Agricultural University. The fish were treated humanely following the regulations of the Administration of Affairs Concerning Experimental Animals for the Science and Technology Bureau of China.

2.2. Source of samples

Broodstock mrigal carp and common carp (*Cyprinus carpio*, CC) were obtained from the State Key Laboratory of Developmental Biology of Freshwater Fish, Human Normal University. During the breeding season, self-crossing and gynogenesis were performed as described in a previous study (Li et al., 2023). GMC was obtained through gynogenesis, and the mature eggs of MC were activated by UV-irradiated sperm of CC. Then, MC and GMC larval fish were carefully reared in two ponds under the same conditions. All the experimental fish were exposed to ambient light concentrations and were fed commercial feed routinely two times a day. The water temperature was 26 ± 2.0 °C and dissolved oxygen was >6.0 mg/L, water pH was 7.0–7.5 and ammonia nitrogen content was 0.02 ± 0.01 mg /L, the nitrite content was 0.02 ± 0.01 mg /L. All the fish were healthy before collection.

2.3. Low-temperature treatments and sampling

For cold stress experiments, the water temperature was set at 14 °C based on our previous study because the critical thermal minimum (CTMin) was detected at 11.65 ± 0.25 °C (Li et al., 2023). Thirty MC and thirty GMC (23.78 ± 4.49 g, 10.82 ± 1.82 cm) were randomly selected and transferred into two tanks of the same size with a temperature-adjustable continuous flow system (Ningbo Jiangnan Instrument Factory, Ningbo, China). The experimental fish were reared at room temperature (26 °C) for 1 week and fed commercial pelleted feed twice a day. After 1 week of acclimation, samples from the MC group (control group, named the CG) were collected. Then, the water temperature of the GMC group started to decline from 26 °C to 14 °C over 36 h at a rate of 0.3 °C/ h. Test Group 1 (TG1) was sampled at this temperature point. Test Group 2 (TG2) was sampled after the fish were maintained at 14 °C for 48 h to explore the effect of longtime low temperature (in 48 h) on GMC fish, if the physiological functions and the genes level were normalized or continue changed. A flowchart of the cold treatments is presented in Fig. S1.

The experimental fish were euthanized with 0.3 mg/L MS-222 before tissue collection, when the fish were out of balance and unconscious, they were transferred into clean dish and wiped off the solution for dissection. In each group (CG, TG1 and TG2), a piece of liver tissue and gill tissue from three individuals was placed into Bouin's fixative for histological analysis. Three liver tissues in each group were collected and soaked in RNAlater at 4 °C for 24 h before storage at −70 °C for RNA-Seq and qPCR. Another 5 liver tissues in each group were collected and temporarily stored in liquid nitrogen and transferred to −70 °C freezer for subsequent metabolome analysis.

2.4. RNA extraction, library construction and sequencing

Total RNA was extracted from liver tissues using the standardized protocol as described in the TRIzol Reagent Kit (Invitrogen). RNA degradation and contamination were determined by 1.0% agarose gel electrophoresis. Total amounts and the integrity of the RNA were assessed using the RNA Nano 6000 Assay Kit of the Bioanalyzer 2100 system (Agilent Technologies, CA, USA). The RNAs were purified by using Agencourt RNAClean XP Beads from Beckman Coulter. Approximately 2 μg of total RNA from each sample was used to construct a cDNA library with the VAHTS Universal V6 RNA-seq Library Prep Kit according to the manufacturer's instructions. Both first and second strand cDNA were synthesized by PCR amplification. Double strand cDNAs were purified using the Agencourt AMPure XP from Beckman Coulter and ligated to adaptors of the NEBNext Multiplex Oligos for Illumina. Finally, Q5 Hot Start HiFi PCR Master Mix (NEB) was used for PCR enrichment of the adaptor-ligated DNA. The concentration and quality of the libraries were measured by using the Agilent High Sensitivity DNA Kit and a Bioanalyzer 2100 from Agilent Technologies. The libraries were sequenced using an Illumina HiSeq 4000 according to the standard Illumina protocols. All libraries were sequenced for 150 nt at both ends.

2.5. Differentially expressed gene identification and functional annotation

Quantification of gene expression levels was calculated by fragments

per kilobase of transcript per million mapped reads (FPKM) (Trapnell et al., 2010). The expression values of three biological replicates were screened with threshold (mean ± 2 standard deviation) in each gene to avoid interference from expression noise (Dillies et al., 2013). Differential expression analysis between two groups was performed using DESeq2 (version 2.13) (Love et al., 2014). The resulting *p* values were adjusted using Benjamini and Hochberg's approach for controlling the false discovery rate (FDR). Genes with an adjusted p values <0.05 and a threshold normalized absolute log 2-fold change >2 were assigned as differentially expressed genes (DEGs).

Gene function was annotated based on seven public databases, namely, NCBI non-redundant protein sequences (Nr), NCBI nonredundant nucleotide sequences (Nt), Protein family (Pfam), Clusters of Orthologous Groups of proteins (COG), Swiss-Prot, KEGG Orthologue database (http://www.genome.jp/kegg/) and Gene Ontology (GO) (http://www.geneontology.org/).

2.6. LC–MS analysis

For metabolite extraction, 100 mg of each liver sample was weighted and homogenized, and the supernatant (250 μL per sample) was collected for LC–MS analysis as previously described (Wen et al., 2019). LC–MS /MS analyses were performed using an ExionLC™ AD system (SCIEX) coupled with a QTRAP® 6500+ mass spectrometer (SCIEX) at Novogene Co., Ltd. (Beijing, China). The supernatant was injected onto an Xselect HSS T3 column (2.1 × 150 mm, 2.5 μm) using a 20-min linear gradient at a flow rate of 0.4 mL/min for the positive/negative polarity mode. The eluents were eluent A (0.1% formic acid-water) and eluent B (0.1% formic acid-acetonitrile) (Luo et al., 2015). The solvent gradient was set as follows: 2% B, 2 min; 2–100% B, 15 min; 100% B, 17 min; 100–2% B, 17.1 min; and 2% B, 20 min. The QTRAP® 6500+ mass spectrometer was operated in positive polarity mode with a curtain gas of 35 psi, collision gas of medium, ion spray voltage of 5500 V, temperature of 550 °C, ion source gas of 1:60, and ion source gas of 2:60.

2.7. Identification of differential metabolites and metabolic pathway analysis

The raw data were processed by SCIEX OS V1.4 software for peak extraction, peak alignment, and other data processing operations. The MS/MS spectra matching score was calculated using the dot-product algorithm taking fragments and intensities into account. The matching score cut-off was set as 0.8. All extracted ion peak areas of the data were normalized, and the data were subjected to Pareto-scaling processing in SICMA-P 14.1 software (Umetrics, Umea, Sweden). Multivariate statistical analysis of metabolites, including principal component analysis (PCA) and partial least squares discriminant analysis (PLS-DA), was carried out to reveal the differences in metabolic patterns in different groups. Hierarchical clustering analysis (HCA) and metabolite correlation analysis were used to reveal the relationship between samples and between metabolites. The variable important for the projection (VIP), fold change (FC) and *P* value were calculated to reveal the metabolite expression patterns for identification and classification. The threshold value was set as VIP value >1.0, FC value >1.5 or FC value <0.667 and P value <0.05 to determine the significantly different metabolites between the pairwise comparison groups (Li et al., 2019a). These metabolites were annotated using the KEGG database (http://www.genome.jp/kegg/) and HMDB database (http://www.hmdb.ca/).

2.8. Integration analysis of the transcriptome and metabolome

Transcriptome and metabolome analyses were combined to identify the regulatory pathways involving differentially expressed genes and metabolites. The relationships among significantly different genes and metabolites were mapped into an interaction network by Cytoscape software to provide rich and comprehensive information for revealing the molecular mechanisms of the response to low-temperature stress at different levels.

2.9. Validation of significant DEGs by RT–qPCR

Total RNA was isolated from liver tissues using TRIzol reagent (Invitrogen) according to the manufacturer's instructions. First-strand cDNA was synthesized using a PrimeScript RT Reagent Kit (RR047A, TAKARA) with PrimeScript RT Enzyme at 37 °C for 15 min and at 85 °C for 5 s after genomic DNA removal with DNA eraser. qPCR was performed on triplicate technical replicates, and the ACTN gene (accession no. GU471241) was used as the internal control for normalization of gene expression. qPCR was performed on a LightCycler® 96 (Roche, Switzerland) and the amplification conditions were as follows: 50 °C for 5 min, 95 °C for 10 min, and 40 cycles at 95 °C for 15 s and 60 °C for 60 s. Then, relative quantification was performed, and melting curve analysis was used to verify the generation of a single product at the end of the assay. The average cycle threshold (Ct) was calculated for each sample using the $2^{-\Delta\Delta Ct}$ method. The sequences of the primers used are given in Table S1.

3. Results

3.1. Histological study of the gill and liver

The gill filament structure of the CG was neatly arranged, completed and compacted (Fig. 1A). After cold stress in the TG1, the terminus of part of the gill filament was enlarged, and mucus cells and their secretions were increased (Fig. 1B). After 48 h of cold acclimation in the TG2, the terminus of the gill filament was significantly enlarged, and there was a further increase in mucus cells and their secretions (Fig. 1C). The hepatocytes of the CG presented normal liver parenchyma that was evenly distributed with complete structure and clear boundaries (Fig. 1D). After cold stress in the TG1, part of the hepatocyte nucleus of GMC was shifted, blurred and disintegrated; the cells became swollen, and vacuoles appeared (Fig. 1E). After 48 h of cold acclimation in the TG2, the number of degenerative hepatocytes was increased (Fig. 1F).

3.2. DEG identification and functional enrichment

A total of 1.9×10^8 clean reads (57.44 Gb) was obtained from 12 liver transcriptomes. Approximately 77.94% of these clean reads were mapped to the reference genomes. Basic information on the transcriptome is presented in Table S2. The complete clean reads were uploaded to the NCBI Sequence Read Archive (SRA) website under accession number PRJNA895734.

Based on the mapped reads and FPKM, DEGs between the control group (CG) and cold stress groups (TG1 and TG2) were identified. A total of 23,378 genes were co-expressed in the CG and TG1, among which 6267 genes were DEGs, including 3118 that were upregulated and 3149 that were downregulated in the TG1 compared with the CG. In contrast, a total of 24,994 genes were co-expressed in the CG and TG2, among which 8338 genes were DEGs, including 4107 that were upregulated and 4231 that were downregulated in the TG2 compared with the CG. In addition, 1691 DEGs were detected between the TG1 and TG2, including 1129 upregulated and 562 downregulated DEGs (Fig. 2A). The top 10 DEGs in the two cold stress groups are presented in Table 1. Interestingly, several upregulated genes including MHC1, AURKA, and SCD, and several downregulated genes including ANG, JDP2, NTNG2, and COL21A were detected in the two cold stress groups of fish.

To better understand the differences between the TG1 and TG2 fish in cold stress, the shared DEGs were identified, and the tendency was analysed. A total of 4867 DEGs were identified in TG1 and TG2, among which 2420 DEGs were upregulated and 2424 DEGs were downregulated (Fig. 2B and C). The shared DEGs were assigned to GO function analysis, with the top 3 upregulated DEG clusters were metabolic

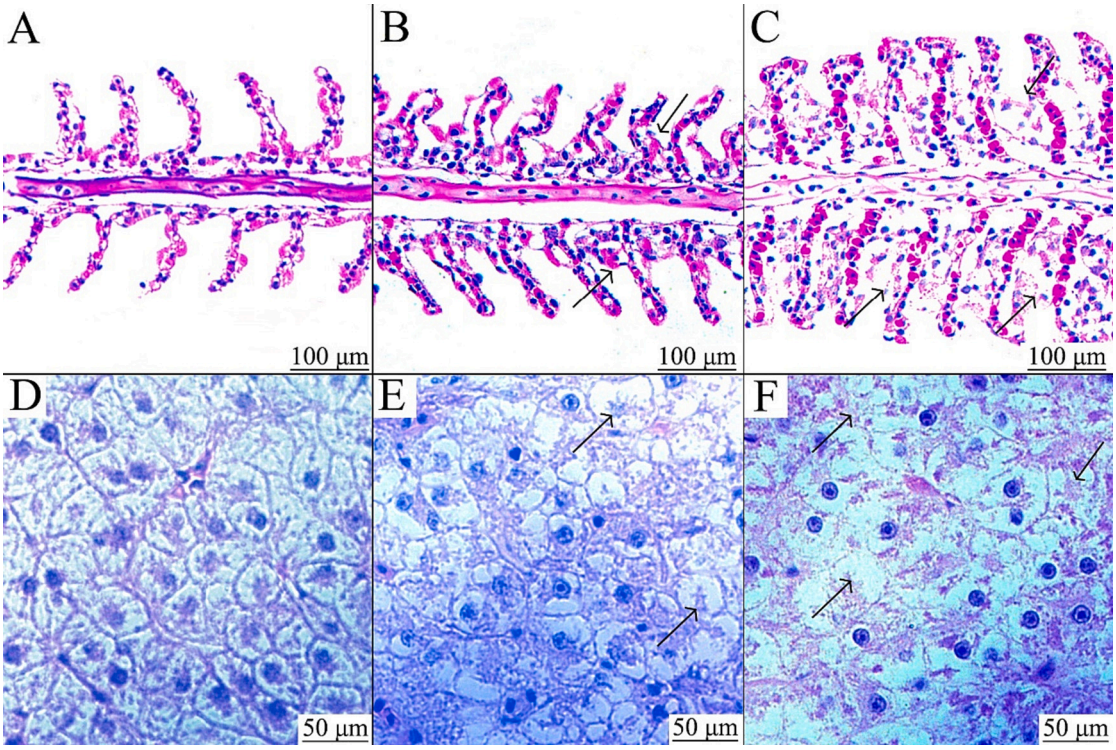

Fig. 1. Microstructure of gill and liver tissues in GMC and MC fish after cold stress. CG group: gill (A) and liver (D) tissues; TG1 group: gill (B) and liver (E) tissues; TG2 group: gill (C) and liver (F) tissues.

process, catalytic activity and organic substance metabolic process, while the top 3 downregulated DEG clusters were extracellular region, extracellular region part and extracellular space (Fig. S2 and Table S3). In the KEGG database, the shared DEGs were classified into 5 major categories with 14 subclasses, and the top 3 subclasses were oxidative phosphorylation (8.95%), proteasome (5.65%) and Parkinson's disease (8.54%). The shared upregulated genes were highly enriched in oxidative phosphorylation, proteasome, and the citrate cycle (TCA cycle) (Fig. 2D), while the downregulated genes were mainly enriched in *Staphylococcus aureus* infection, systemic lupus erythematosus, and leishmaniasis. (Fig. 2E). The expression trend of the shared DEGs can be divided into 7 patterns, and most DEGs were categorized into two expression patterns: gradually increasing (1933 genes) and gradually decreasing (1830 genes) (Fig. 3).

3.3. Metabolite identification and functional enrichment

To better understand the effects of cold stress on liver metabolism, metabolites were detected between CG and TG2 fish. The PCA results showed that the CG and TG2 fish were completely separated, which was the basis for subsequent screening of differential metabolites (Fig. 4A). Based on the three parameters of the VIP, FC, and *P* value, 767 metabolites were identified in the CG and TG2, among which 160 metabolites were DMs, including 39 that were increased and 121 that were reduced (Fig. 4B). The top 20 DMs are listed in Table 2. HMDB classification revealed that the DMs were mainly classed into lipids and lipid-like molecules, organic acids and derivatives and organoheterocyclic compounds (Table S4). Correlation analysis of DMs between the CG and TG2 showed that most of the top 20 DMs were positively correlated (Fig. 4C).

KEGG pathway annotation revealed that the largest pathways with >50 metabolites were amino acid metabolism, carbohydrate metabolism, metabolism of cofactors and vitamins, and nucleotide metabolism (Fig. S3). The identified DMs were mainly enriched in retinol metabolism, folate biosynthesis, and histidine metabolism pathways (Fig. 5).

3.4. Co-analysis of DMs and DEGs

To determine the shared pathway between all DMs and DEGs, they were mapped to the KEGG pathway database, and the result is shown in Fig. 6. The top 5 common pathways were oxidative phosphorylation (2 Meta, 78 Tran), purine metabolism (8 Meta, 71 Tran), neuroactive ligand–receptor interaction (4 Meta, 36 Tran), galactose metabolism (5 Meta, 11 Tran) and histidine metabolism (6 Meta, 9 Tran) (Fig. 6A). For insight into the relationship between DMs and DEGs in common pathways, we conducted a correlation analysis on DMs and DEGs. GMP in purine metabolism was positively correlated with 4 DEGs (C3, ALDH, MHC2 and CFB) and had no relation with the other 4 DEGs, guanine and inosine were positively correlated with 6 DEGs, and the other DMs were negatively correlated with most DEGs (Fig. 6B). For retinol metabolism and folate biosynthesis, Prpp was negatively correlated with all DEGs, and Sepiapterin, 4-Ab, atRAL and 4-oxoROL were all positively correlated (Fig. 6C).

3.5. Validation of the main DEGs by qPCR

To validate the quality of the RNA-seq data, we randomly chose 8 DEGs involved in metabolism and growth (cold-inducible RNA-binding protein (CIRBP), nuclear respiratory factor 1 (NRF1), stearoyl-CoA desaturase (SCD), elongation of very long chain fatty acids protein 2 (ELOVL2), hydroxymethylglutaryl-CoA reductase (NADPH) (HMGCR), fibulin 7 (FBLN7), angiogenin (ANG), and fibroblast growth factor (FGF)) to perform qPCR. The relative expression levels of the 8 DEGs are presented in Fig. 7. The trends of the expression levels of these genes detected by qPCR were the same as those obtained by RNA-seq data analysis. These results indicated the reliability of the RNA-seq data for the analysis of differentially expressed genes in this study.

4. Discussion

Fish acclimation to cold stress is accompanied by changes in

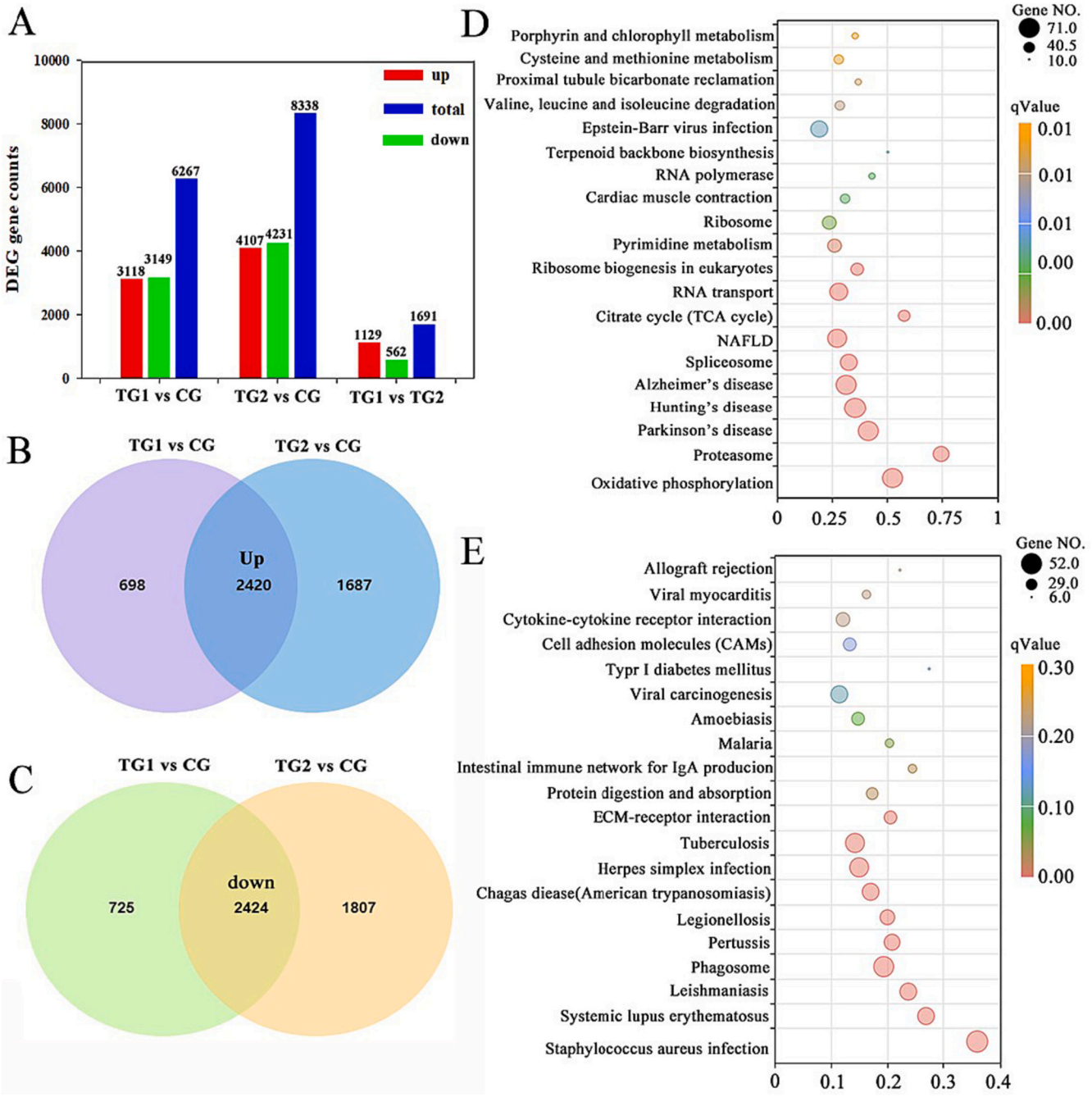

Fig. 2. Identification and function enrichment of the DEGs in the two cold stress group fish. (A), the number of DEGs in the three groups of fish, red represents the upregulated genes, green represents the downregulated genes; blue represents the total DEGs. (B) Veen showed the upregulated DEGs that shared in the two cold stress group fish. (C) Veen showed the downregulated DEGs that shared in the two cold stress group fish. (D) KEGG enrichment analysis of the upregulated DEGs in two comparison groups. (E) KEGG enrichment of the downregulated DEGs in two comparison groups. Three comparison groups include TG1 vs CG, TG2 vs CG, TG1 vs TG2, respectively. (For interpretation of the references to color in this figure legend, the reader is referred to the web version of this article.)

apparatus and tissue structure. The apoptotic cells in the gill were significantly increased at 1–3 h in zebrafish after cold shock at 12 °C, while the liver cells appeared slightly apoptotic at 3 h and increased to a higher level at 6 h (Wu et al., 2015). In *Nibea albiflora*, after cold stress at 13 °C for 24 h, the gill tissue showed shrinkage membrane contraction and even fracture, while severe fatty degeneration and cavitation were induced in the hepatocytes (Song et al., 2019). Similar results were observed in this study. After cold stress, the gill filament was enlarged, and the nuclei of hepatocytes were shifted and disintegrated. Interestingly, no break in gill filaments was observed, but mucus secretion was significantly increased (Fig. 1), suggesting that the increase in mucus may be a compensatory mechanism for adapting to cold stress.

Energy balance plays a vital role in the ability of fish to make physiological adjustments to the cold environment, particularly the pathways associated with energy (Nitzan et al., 2019). Oxidative phosphorylation is the main pathway for ATP production, which was significantly active in *Larimichthy crocea* treated at 9 °C for 12 h (Qian and Xue, 2016). In *Takifugu obscurus*, the DEGs in oxidative phosphorylation were significantly increased after a linear cooling scheme at 16 °C (Han et al., 2022). The citrate cycle (TCA cycle) provides the substrate for oxidative phosphorylation, and it plays a crucial role in energy metabolism, which has been proven to be associated with cold

Table 1
Top 10 DEGs in TG1 and TG2 compared with CG groups fish.

TG1 vs CG			TG2 vs CG		
KO	Gene	Log2 (fold change)	KO	Gene	Log2 (fold change)
K06751	MHC1	10.119	K00489	CYP7A1	10.259
K11481	AURKA	9.5724	K15261	PARP10	10.139
K13703	ABHD11	8.1125	K06751	MHC1	9.4913
K15728	LPIN	8.0826	K00507	SCD	8.6662
K00507	SCD	8.0351	K00485	FMO	8.6338
K00626	atoB	7.8098	K11481	AURKA	8.4829
K00671	NMT	7.6244	K12009	TRIM27	8.383
K17442	FOG2	7.5595	K02996	MRPS9	8.2611
K13649	FOLR	7.481	K10661	DOA10	8.1548
K14282	TACC2	7.454	K14012	SHP1	7.9483
K16631	ANG	−9.3608	K17342	FBLN7	−10.934
K09033	JDP2	−8.6254	K16631	ANG	−9.8477
K15103	UCP2	−8.6233	K09033	JDP2	−9.1124
K13863	SLC7A1	−8.6178	K16359	NTNG2	−8.8936
K12474	LDLRAP1	−8.2677	K02184	FMN2	−8.1934
K05736	PAK7	−7.9532	K12474	LDLRAP1	−7.7924
K04360	NTRK2	−7.6833	K16629	COL21A	−7.7923
K15261	PARP10	−7.47	K09029	FOSB	−7.7808
K16359	NTNG2	−7.4451	K12837	U2AF2	−7.6674
K16629	COL21A	−7.3056	K19930	SRCIN1	−7.5189

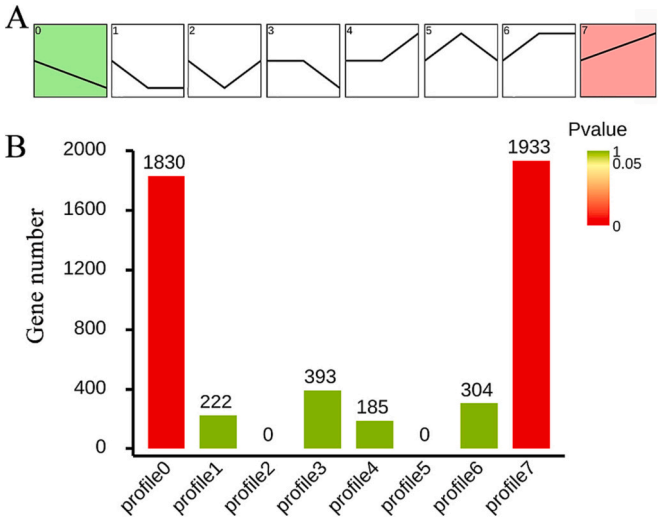

Fig. 3. Analysis on the trend of shared DEGs in CG, TG1 and TG2 groups of fish. (A), seven expression patterns of the DEGs; (B), distribution of the seven expression patterns. Profile 0–7 represents seven expression patterns of DEGs.

adaptation and development in *Schizothorax prenanti* (Li et al., 2019b). In *Nibea albiflora*, the TCA cycle pathway was significantly enriched after cold stress at 12.7 °C for 5 h (Song et al., 2019). The DEGs enriched in oxidative phosphorylation and TCA cycle were also upregulated in our study (Fig. 2). These results suggested that high energy levels are required for GMC survival under cold stress. Moreover, other representative pathways involved in energy, immunity and disease, such as proteasome and FoxO signalling pathway, were also upregulated in GMC (Fig. 2). The proteasome is crucial for maintaining protein homeostasis, has proven to be one of the most representative pathways for resistance to cold acclimation in zebrafish (Todgham et al., 2017). The FoxO signalling pathway is involved in apoptosis, oxidative stress resistance and immune regulation in several fishes (Hu et al., 2016; Wang et al., 2023). Interestingly, the number of DEGs during the cooling period (TG1 vs. CG) was greater than the cryogenic maintenance period (TG2 vs. TG1), suggesting the transcription was rapidly activated in response to cold stress, and then the GMC could gradually recover, and the transcriptome response gradually tend to normalize (Fig. 3).

Cold stress causes a severe reduction in immune defense and disease resistance, and these effects are significantly reflected in genes and pathways (Abram et al., 2017). In *Nibea albiflora*, after cold stimulation at 13 °C for 1 h, staphylococcus aureus infection and leishmaniasis pathways were identified, demonstrating the adverse effects of cold stress on immunity and disease (Song et al., 2019). Similarly, systemic lupus erythematosus and pertussis were identified in *Trachinotus ovatus* and *Epinephelus coioides* under cold conditions (Han et al., 2021; Sun et al., 2019b). These pathways were also downregulated in GMC (Fig. 2), indicating that immune defense and disease resistance were obviously decreased to cope with cold stress. Furthermore, many DEGs associated with immunity and disease were also identified (Table 1). MHC1(major histocompatibility complex —I) plays a vital role in the initiation and regulation of the immune response, and AURKA (aurora a kinase) is related to inflammation and tumorigenesis. The upregulated of MHC1 and AURKA indicated the occurrence of inflammation and the response of immune mechanisms (Robledo et al., 2014; Su et al., 2019). Downregulated genes, such as ANG (angiopoietin), JDP2 (jun dimerization protein 2) and COL21A (collagen type XXI alpha 1 chain), in GMC are involved in maintaining a normal physiological state, and resisting inflammation and diseases (Mansour et al., 2018; Matsumoto et al., 2012).

Metabolomics has been suggested to be an effective tool for detecting metabolite fluctuations in response to environmental stressors (Chen et al., 2021). The liver is the central organ of energy metabolism and is most responsive to energy changes (Robledo et al., 2014). In this study, the DMs associated with carbohydrate, fat and amino acid metabolism were evidently reduced (Tables 2 and S4), suggesting that energy expenditure or turnover was increased and energy was rapidly depleted in GMC during cold stress (Wen et al., 2018). Meanwhile, phospholipids were significantly reduced, revealing that GMC adapts to the cold environment by reducing membrane fluidity and diluting material exchange between cells (Liu et al., 2022). Moreover, there were three pathways significantly enriched in our study (Fig. 5). Folate biosynthesis has essential effects on fish growth and reproduction, which is also detected as an effective pathway to activating the immune system in *Macrobrachium nipponense* (Xu et al., 2016; Zhu et al., 2020). Histidine metabolism is sensitive to cold reactions and may have critical roles in regulating adversity development, which was significantly increased in *Dicentrarchus labrax* after hypothermia maintenance, indicating its crucial role in compensatory growth (Brosnan and Brosnan, 2020; Zhang et al., 2021). Retinol metabolism dysfunction might contribute to the lower visual ability in *Siniperca chuatsi* and be involved in the immune and antioxidant systems in *Takifugu fasciatus* after cold stress at 12 °C for 24 h. (He et al., 2021; Wen et al., 2019). In this study, the significant enrichment of these pathways indicates that they may be the key pathways in GMC during cold tolerance. However, the functions of these metabolites need further investigation.

Correlation analysis of the metabolome and transcriptome can provide an overall understanding of the effect of cold stimulation on fish. Oxidative phosphorylation is a multistep process of mitochondrial energy generation involving several integrated reactions influenced by temperature and is an essential way for fish to resist cold stress (Baris et al., 2016). Purine metabolism has been found to be highly involved in the metabolic response to cold stress, and purines play a protective role after stress or injury, potentially regulating immune responses (Jiao et al., 2020; Kuo et al., 2022). The dynamic remodeling of the actin cytoskeleton is a critical part of most cellular activities, and it has important effects on the activities of fish cells, and malfunction of cytoskeletal proteins results in various diseases (Adam et al., 2019). Moreover, many shared pathways in the transcriptome and metabolism were identified (Fig. 6). These pathways are closely related to the individual's immunity, metabolism and growth, further confirming that the impact of cold on fish is multifaceted. However, the function of these DEGs and DMs requires further investigation.

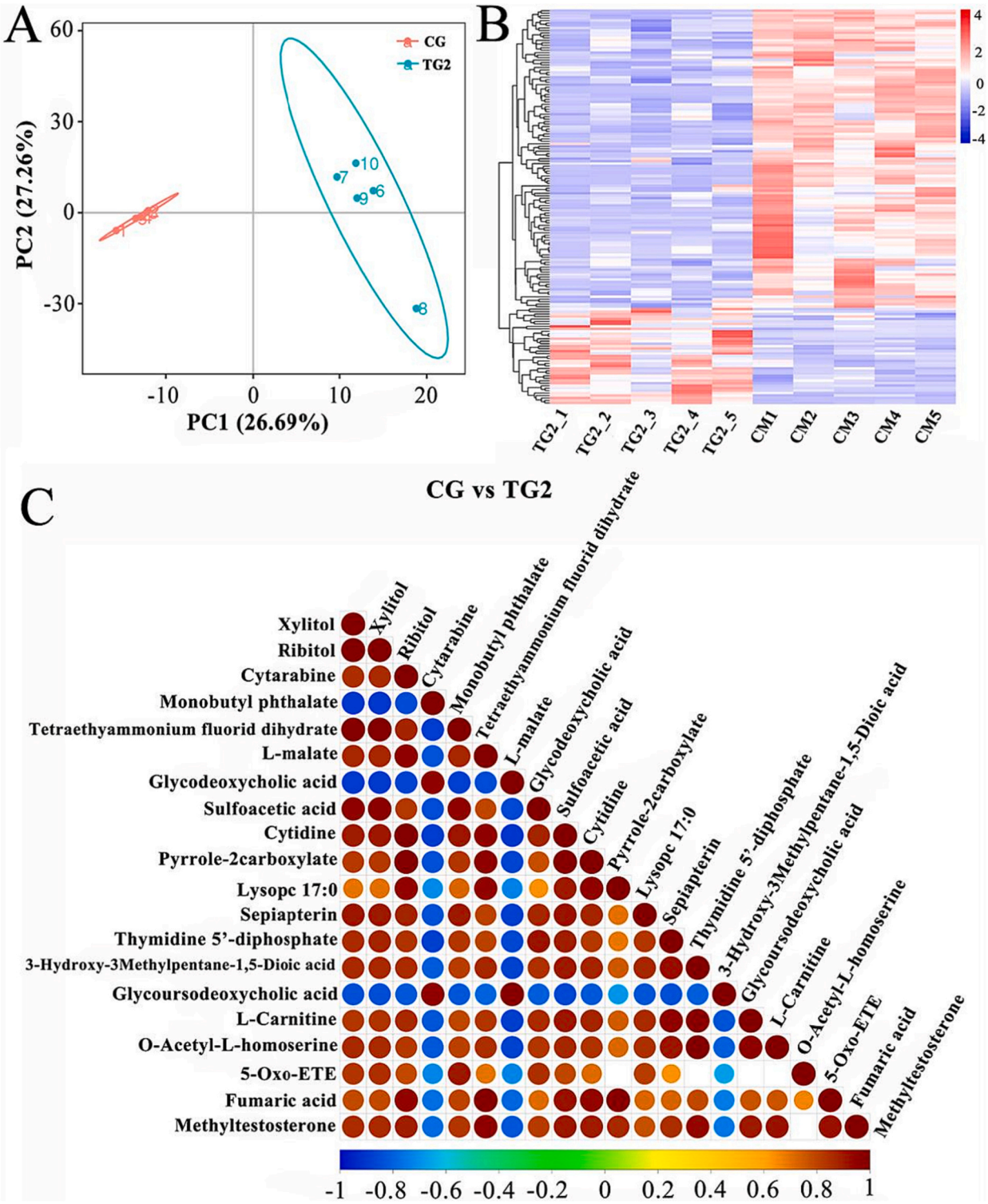

Fig. 4. Identification and correlation analysis of DMs in the two cold stress groups of fish. A: PLS-DA score scatter chart and sequence verification chart. B: Cluster thermogram of grouping difference metabolites, the vertical is the clustering of samples, and the horizontal is the clustering of metabolites. C: Correlation diagram of top 20 DMs, red indicates full positive correlation, blue indicates full negative correlation, and the part without color indicates P value>0.05. (For interpretation of the references to color in this figure legend, the reader is referred to the web version of this article.)

5. Conclusion

This study suggests that cold stress resulted in marked changes in the transcriptome and metabolome of GMC livers. Under cold stress, the transcriptome of the GMC liver was significantly active at first and then was modified, suggesting that the GMC entered a state of hypothermia, and most transcriptomic changes were related to energy metabolism, immunity and disease, and cell homeostasis. The metabolomics results suggested that energy metabolism was the most affected, and GMC adapted to a low water temperature environment by reducing energy consumption. In addition, fat metabolism, histidine metabolism and some immune-related pathways were also affected. Overall, the results

Table 2
Top 20 DMs between CM and GMC groups fish under cold stress.

Name	Class	VIP	FC	P value	Regulation
Xylitol	Sugar alcohols	1.96	0.009	0.0000000001	reduce
Ribitol	Sugar alcohols	1.96	0.008	0.000000001	reduce
Cytarabine	Nucleotide and its derivates	1.95	0.007	0.000000003	reduce
Monobuty l phthalate	Organic acid and its derivatives	1.95	188.639	0.000000003	increase
Tetraethylammonium fluoride dihydrate	Nucleotide and its derivates	1.95	0.008	0.00000002	reduce
L-Malate	Tca cycle	1.92	0.015	0.000001	reduce
Glycodeoxycholic acid	Bile acids	1.91	6.106	0.000002	increase
Sulfoacetic acid	Organic acid and its derivatives	1.91	0.174	0.000003	reduce
Cytidine	Nucleotide and its derivates	1.94	0.008	0.000004	reduce
Pyrrole-2-carboxylate	Organoheterocyclic compounds	1.94	0.066	0.000004	reduce
Lysopc 17:0	Phospholipid	1.88	0.043	0.00001	reduce
Sepiapterin	Organoheterocyclic compounds	1.87	0.611	0.00001	reduce
Thymidine 5′-diphosphate	Nucleotide and its derivates	1.87	0.379	0.00003	reduce
3-Hydroxy-3-Methylpentane-1,5-Dioic Acid	Fatty acyls	1.85	0.589	0.00005	reduce
Glycoursodeoxycholic acid	Bile acids	1.84	7.154	0.00007	increase
L-Carnitine	Carnitine	1.84	0.584	0.0001	reduce
O-Acetyl-L-homoserine	Amino acid and Its derivatives	1.81	0.587	0.0001	reduce
5-Oxo-ETE	Fatty acyls	1.81	0.137	0.0001	reduce
Fumaric acid	TCA cycle	1.84	0.033	0.0001	reduce
Methyltestosterone	Hormones	1.81	0.256	0.0002	reduce

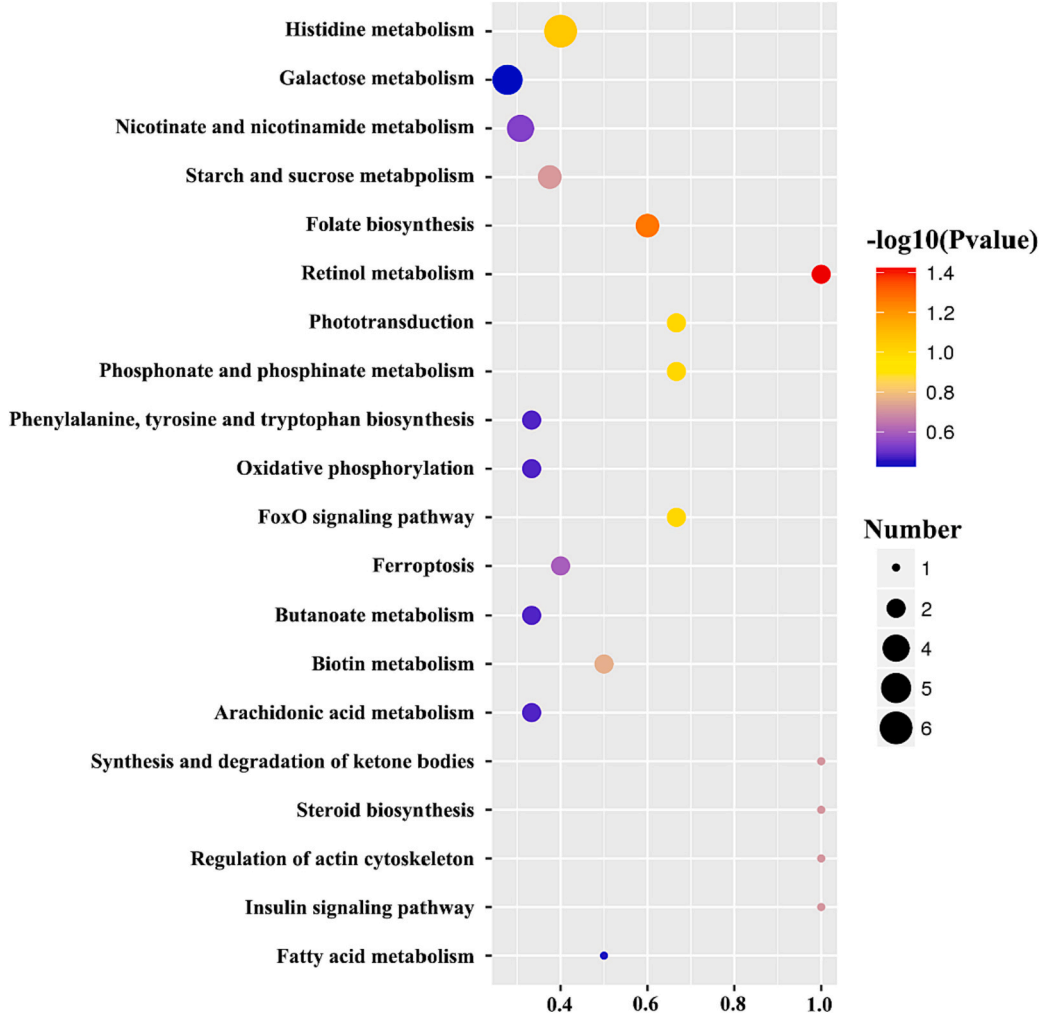

Fig. 5. KEGG enrichment of DMs in CG and TG2 groups fish. The color of the point represents the *P*-value of the hypergeometric test, and the size of the point represents the number of differential metabolites in the corresponding pathway.

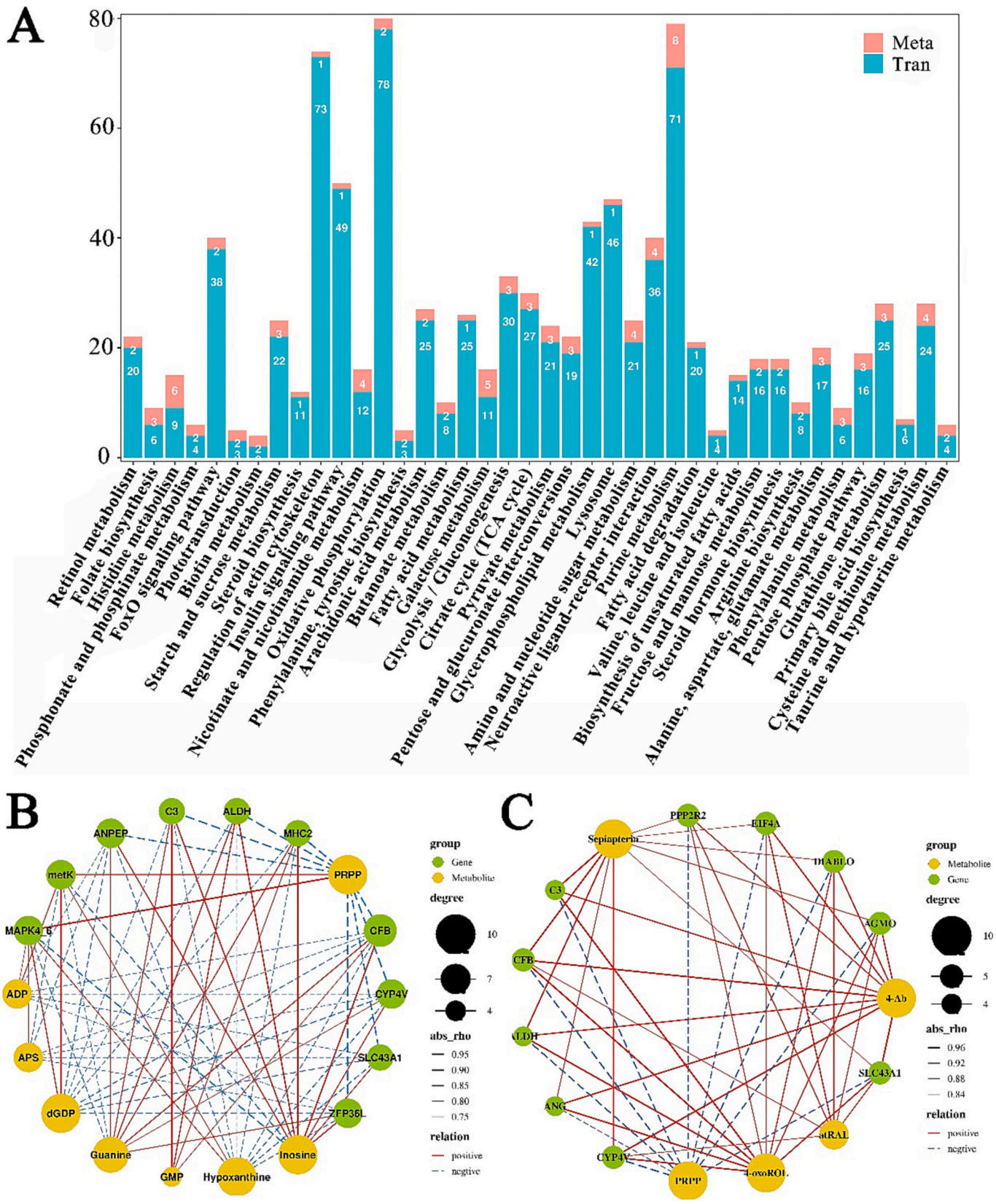

Fig. 6. Co-analysis of DEGs and DMs between CG and cold stress groups fish.
(A), The shared pathway between all DMs and DEGs, (B), Correlation analysis of DEGs and DMs in retinol metabolism & folate biosynthesis pathway, (C), Correlation analysis of DEGs and DMs in purine metabolism.

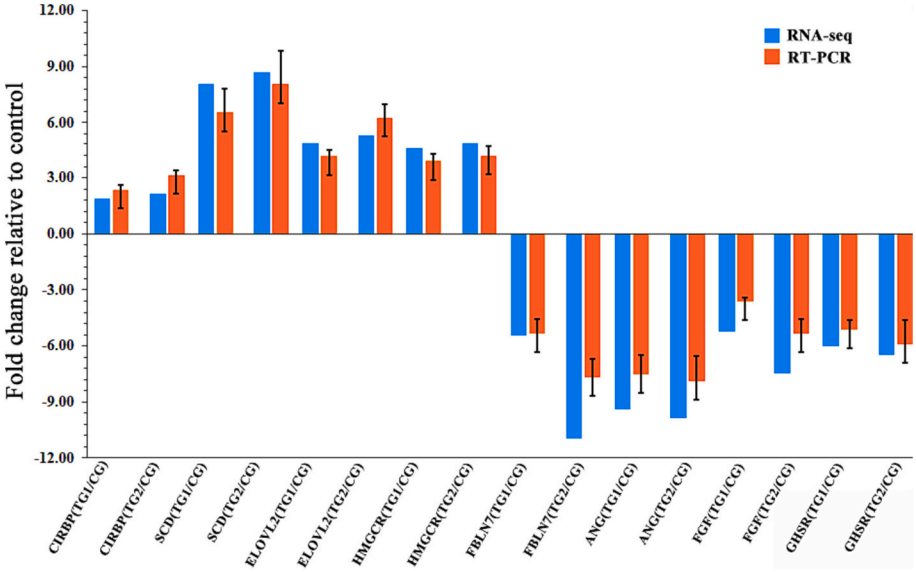

Fig. 7. Validation of RNA-Seq results using RT-PCR. The transcript expression levels of the selected genes were normalized to that of the β-actin gene.

of transcriptomics and metabolomics provided insights into the physiological regulation in response to cold stress.

Author statement

Author 1 (First Author): Hongqing Li	Conceived the study, designed the experiments, performed experimental work, wrote and modified the manuscript.
co-first authors: Wuhui Li	Performed experimental work, and collected samples.
co-first authors: Jisen Su	Performed experimental work, and collected samples.
Author 2: Zexun Zhou	Performed experimental work.
Author 3: Yan Miao	Performed experimental work.
Author 4: Xuelei Tian	Performed experimental work.
Author 5: Min Tao	Modified this manuscript.
Author 6: Chun Zhang	Modified this manuscript.
Author 7: Yi Zhou	Modified this manuscript.
Author 8: Qinbo Qin	Modified this manuscript.
Author 9 (Corresponding Author 1):Huirong Yang	Conceived the study, designed the experiments, performed experimental work, wrote and modified the manuscript.
Author 10a (Corresponding Author 2): Shaojun Liu	Conceived the study, designed the experiments, performed experimental work, wrote and modified the manuscript.

Declaration of Competing Interest

The authors declare that they have no known competing financial interests or personal relationships that could have appeared to influence the work reported in this paper.

Data availability

Data will be made available on request.

Acknowledgements

This work was supported by the Laboratory of Lingnan Modern Agriculture Project (NT2021008), the National Natural Science Foundation of China (Grant Nos., 32202906, U19A2040), the Natural Science Foundation of Hunan Province (Grant No. 2022JJ40268), earmarked fund for Agriculture Research System of China (Grant No. CARS-45). Provincial Science and Technology Special Fund Project for Zhongshan City (Major Special Project + Task List Management Mode) (2021SDR003, 2022SDR001)

Appendix A. Supplementary data

Supplementary data to this article can be found online at https://doi.org/10.1016/j.aquaculture.2023.740200.

References

Abram, Q.H., Dixon, B., Katzenback, B.A., 2017. Impacts of low temperature on the teleost immune system. Biology 6, 39. https://doi.org/10.3390/biology6040039.

Adam, Moh A., Maftuch, M., Kilawati, Y., Risjani, Y., 2019. The effect of cadmium exposure on the cytoskeleton and morphology of the gill chloride cells in juvenile mosquito fish (*Gambusia affinis*). Egypt. J. Aquat. Res. 45, 337–343. https://doi.org/10.1016/j.ejar.2019.11.011.

Atwood, H.L., Tomasso, J.R., Webb, K., Gatlin III, D.M., 2003. Low-temperature tolerance of Nile tilapia, *Oreochromis niloticus*: effects of environmental and dietary factors. Aquac. Res. 34, 241–251. https://doi.org/10.1046/j.1365-2109.2003.00811.x.

Baris, T.Z., Crawford, D.L., Oleksiak, M.F., 2016. Acclimation and acute temperature effects on population differences in oxidative phosphorylation. Am. J. Phys. Regul. Integr. Comp. Phys. 310, R185–R196. https://doi.org/10.1152/ajpregu.00421.2015.

Brosnan, M.E., Brosnan, J.T., 2020. Histidine metabolism and function. J. Nutr. 150, 2570S–2575S. https://doi.org/10.1093/jn/nxaa079.

Chen, Z., Cheng, C.-H.C., Zhang, J., Cao, L., Chen, Lei, Zhou, L., Jin, Y., Ye, H., Deng, C., Dai, Z., Xu, Q., Hu, P., Sun, S., Shen, Y., Chen, Liangbiao, 2008. Transcriptomic and genomic evolution under constant cold in Antarctic notothenioid fish. Proc. Natl. Acad. Sci. 105, 12944–12949. https://doi.org/10.1073/pnas.0802432105.

Chen, X., Hou, X., Yang, M., Wang, Jingan, Yin, J., Han, H., Wang, Jun, Wang, C., 2021. Differential metabolomic profiles of two closely related Leuciscinae fish, the species Ctenopharyngodon idellus and *Leuciscus idus*. Aquac. Rep. 20, 100650 https://doi.org/10.1016/j.aqrep.2021.100650.

Dillies, M.-A., Rau, A., Aubert, J., Hennequet-Antier, C., Jeanmougin, M., Servant, N., Keime, C., Marot, G., Castel, D., Estelle, J., Guernec, G., Jagla, B., Jouneau, L., Laloë, D., Le Gall, C., Schaëffer, B., Le Crom, S., Guedj, M., Jaffrézic, F., on behalf of The French StatOmique Consortium, 2013. A comprehensive evaluation of normalization methods for Illumina high-throughput RNA sequencing data analysis. Brief. Bioinform. 14, 671–683. https://doi.org/10.1093/bib/bbs046.

Ge, G., Long, Y., Shi, L., Ren, J., Yan, J., Li, C., Li, Q., Cui, Z., 2020. Transcriptomic profiling revealed key signaling pathways for cold tolerance and acclimation of two carp species. BMC Genomics 21, 1–15. https://doi.org/10.1186/s12864-020-06946-8.

Ghisaura, S., Pagnozzi, D., Melis, R., Biosa, G., Slawski, H., Uzzau, S., Anedda, R., Addis, M.F., 2019. Liver proteomics of gilthead sea bream (*Sparus aurata*) exposed to cold stress. J. Therm. Biol. 82, 234–241. https://doi.org/10.1016/j.jtherbio.2019.04.005.

Han, M., Yang, R., Chen, X., Fu, Z., Ma, Z., Yu, G., 2021. Transcriptional response of golden pompano *Trachinotus ovatus* larvae to cold and heat stress. Aquac. Rep. 20, 100755 https://doi.org/10.1016/j.aqrep.2021.100755.

Han, S., Wei, S., Chen, R., Ni, M., Chen, L., 2022. Tissue-specific and differential cold responses in the domesticated cold tolerant Fugu. Fishes 7, 159. https://doi.org/10.3390/fishes7040159.

He, S., You, J.-J., Liang, X.-F., Zhang, Z.-L., Zhang, Y.-P., 2021. Transcriptome sequencing and metabolome analysis of food habits domestication from live prey fish to artificial diets in mandarin fish (*Siniperca chuatsi*). BMC Genomics 22, 1–12. https://doi.org/10.1186/s12864-021-07403-w.

Hu, P., Liu, M., Liu, Y., Wang, Jinfeng, Zhang, Dong, Niu, H., Jiang, S., Wang, Jian, Zhang, Dongsheng, Han, B., Xu, Q., Chen, L., 2016. Transcriptome comparison reveals a genetic network regulating the lower temperature limit in fish. Sci. Rep. 6, 28952. https://doi.org/10.1038/srep28952.

Islam, M.J., Kunzmann, A., Slater, M.J., 2022. Responses of aquaculture fish to climate change-induced extreme temperatures: a review. J. World Aquacult. Soc. 53, 314–366. https://doi.org/10.1111/jwas.12853.

Jiang, H., Lv, W., Wang, Y., Qian, Y., Wang, C., Sun, N., Fang, C., Irwin, D.M., Gan, X., He, S., Yang, L., 2023. Multi-omics investigation of freeze tolerance in the Amur sleeper, an aquatic ectothermic vertebrate. Mol. Biol. Evol. 40 https://doi.org/10.1093/molbev/msad040 msad040.

Jiao, S., Nie, M., Song, H., Xu, D., You, F., 2020. Physiological responses to cold and starvation stresses in the liver of yellow drum (*Nibea albiflora*) revealed by LC-MS metabolomics. Sci. Total Environ. 715, 136940 https://doi.org/10.1016/j.scitotenv.2020.136940.

Johnson, A.C., Turko, A.J., Klaiman, J.M., Johnston, E.F., Gillis, T.E., 2014. Cold acclimation alters the connective tissue content of the zebrafish (*Danio rerio*) heart. J. Exp. Biol. 217, 1868–1875. https://doi.org/10.1242/jeb.101196.

Kuo, C.-H., Ballantyne, R., Huang, P.-L., Ding, S., Hong, M.-C., Lin, T.-Y., Wu, F.-C., Xu, Z.-Y., Chiu, K., Chen, B., Liu, C.-H., 2022. Sarcodia suae modulates the immunity and disease resistance of white shrimp *Litopenaeus vannamei* against *Vibrio alginolyticus* via the purine metabolism and phenylalanine metabolism. Fish Shellfish Immunol. 127, 766–777. https://doi.org/10.1016/j.fsi.2022.07.011.

Li, Z., Liang, H.-W., Luo, X.-Z., Pan, G.-B., Zou, G.-W., 2015. A consecutive self-proliferate silver carp (*Hypophthalmichthys molitrix*) variety created through artificial meiotic gynogenesis. Aquaculture 437, 21–29. https://doi.org/10.1016/j.aquaculture.2014.11.007.

Li, C., Zhang, J., Wu, R., Liu, Y., Hu, X., Yan, Y., Ling, X., 2019a. A novel strategy for rapidly and accurately screening biomarkers based on ultraperformance liquid chromatography-mass spectrometry metabolomics data. Anal. Chim. Acta 1063, 47–56. https://doi.org/10.1016/j.aca.2019.03.012.

Li, R., Zhang, R., Yi, J., Guo, W., Cheng, Q., Zhi, L., Lin, Y., 2019b. Characterization and expression profiles of muscle transcriptome in Schizothoracine fish, *Schizothorax prenanti*. Gene 685, 156–163. https://doi.org/10.1016/j.gene.2018.10.070.

Li, W., Zhou, Z., Tian, X., Li, H., Su, J., Liu, Q., Wu, P., Wang, S., Hu, J., Shen, Z., Zeng, L., Tao, M., Zhang, C., Qin, Q., Liu, S., 2023. Gynogenetic *Cirrhinus mrigala* produced using irradiated sperm of *Cyprinus carpio* exhibit better cold tolerance. Reprod. Breed. 3, 8–16. https://doi.org/10.1016/j.repbre.2023.01.001.

Little, A.G., Loughland, I., Seebacher, F., 2020. What do warming waters mean for fish physiology and fisheries? J. Fish Biol. 97, 328–340. https://doi.org/10.1111/jfb.14402.

Liu, L., Zhang, R., Wang, X., Zhu, H., Tian, Z., 2020. Transcriptome analysis reveals molecular mechanisms responsive to acute cold stress in the tropical stenothermal fish tiger barb (*Puntius tetrazona*). BMC Genomics 21, 737. https://doi.org/10.1186/s12864-020-07139-z.

Liu, Y., Muniz, M.M.M., Lam, S., Song, D., Zhang, Y., Yin, J., Cánovas, A., Liu, H., 2021. Gene expression profile of the taimen *Hucho taimen* in response to acute temperature changes. Comp. Biochem. Physiol. D: Genom. Proteom. 38, 100824 https://doi.org/10.1016/j.cbd.2021.100824.

Liu, M., Zhou, Y., Guo, X., Wei, W., Li, Z., Zhou, L., Wang, Z., Gui, J., 2022. Comparative transcriptomes and metabolomes reveal different tolerance mechanisms to cold stress in two different catfish species. Aquaculture 560, 738543. https://doi.org/10.1016/j.aquaculture.2022.738543.

Love, M.I., Huber, W., Anders, S., 2014. Moderated estimation of fold change and dispersion for RNA-seq data with DESeq2. Genome Biol. 15, 1–21. https://doi.org/10.1186/s13059-014-0550-8.

Luo, P., Dai, W., Yin, P., Zeng, Z., Kong, H., Zhou, L., Wang, X., Chen, S., Lu, X., Xu, G., 2015. Multiple reaction monitoring-ion pair finder: a systematic approach to transform nontargeted mode to pseudotargeted mode for metabolomics study based on liquid chromatography–mass spectrometry. Anal. Chem. 87, 5050–5055. https://doi.org/10.1021/acs.analchem.5b00615.

Manan, H., Noor Hidayati, A.B., Lyana, N.A., Amin-Safwan, A., Ma, H., Kasan, N.A., Ikhwanuddin, M., 2022. A review of gynogenesis manipulation in aquatic animals. Aquac. Fish. 7, 1–6. https://doi.org/10.1016/j.aaf.2020.11.006.

Mansour, M.R., He, S., Li, Z., Lobbardi, R., Abraham, B.J., Hug, C., Rahman, S., Leon, T. E., Kuang, Y.-Y., Zimmerman, M.W., Blonquist, T., Gjini, E., Gutierrez, A., Tang, Q., Garcia-Perez, L., Pike-Overzet, K., Anders, L., Berezovskaya, A., Zhou, Y., Zon, L.I., Neuberg, D., Fielding, A.K., Staal, F.J.T., Langenau, D.M., Sanda, T., Young, R.A., Look, A.T., 2018. JDP2: an oncogenic bZIP transcription factor in T cell acute lymphoblastic leukemia. J. Exp. Med. 215, 1929–1945. https://doi.org/10.1084/jem.20170484.

Matsumoto, T., Deguchi, T., Kawasaki, T., Yuba, S., Sato, J., 2012. Molecular cloning and expression of the col2a1a and col2a1b genes in the medaka, *Oryzias latipes*. Gene Expr. Patterns 12, 46–52. https://doi.org/10.1016/j.gep.2011.11.002.

Mitrovic, D., Perry, S.F., 2009. The effects of thermally induced gill remodeling on ionocyte distribution and branchial chloride fluxes in goldfish (*Carassius auratus*). J. Exp. Biol. 212, 843–852. https://doi.org/10.1242/jeb.025999.

Nitzan, T., Kokou, F., Doron-Faigenboim, A., Slosman, T., Biran, J., Mizrahi, I., Zak, T., Benet, A., Cnaani, A., 2019. Transcriptome analysis reveals common and differential response to low temperature exposure between tolerant and sensitive blue Tilapia (*Oreochromis aureus*). Front. Genet. 10.

Panase, P., Saenphet, S., Saenphet, K., 2018. Biochemical and physiological responses of Nile tilapia *Oreochromis niloticus* Lin subjected to cold shock of water temperature. Aquac. Rep. 11, 17–23. https://doi.org/10.1016/j.aqrep.2018.05.005.

Qian, B., Xue, L., 2016. Liver transcriptome sequencing and de novo annotation of the large yellow croaker (Larimichthy crocea) under heat and cold stress. Mar. Genomics 25, 95–102. https://doi.org/10.1016/j.margen.2015.12.001.

Reid, C.H., Patrick, P.H., Rytwinski, T., Taylor, J.J., Willmore, W.G., Reesor, B., Cooke, S. J., 2022. An updated review of cold shock and cold stress in fish. J. Fish Biol. 100, 1102–1137. https://doi.org/10.1111/jfb.15037.

Robledo, D., Ronza, P., Harrison, P.W., Losada, A.P., Bermúdez, R., Pardo, B.G., José Redondo, M., Sitjà-Bobadilla, A., Quiroga, M.I., Martínez, P., 2014. RNA-seq analysis reveals significant transcriptome changes in turbot (*Scophthalmus maximus*) suffering severe enteromyxosis. BMC Genomics 15, 1149. https://doi.org/10.1186/1471-2164-15-1149.

Schleger, I.C., Pereira, D.M.C., Resende, A.C., Romão, S., Herrerias, T., Neundorf, A.K.A., Sloty, A.M., Guimarães, I.M., de Souza, M.R.D.P., Carster, G.P., Donatti, L., 2022. Cold and warm waters: energy metabolism and antioxidant defenses of the freshwater fish Astyanax lacustris (Characiformes: Characidae) under thermal stress. J. Comp. Physiol. B. 192, 77–94. https://doi.org/10.1007/s00360-021-01409-2.

Song, H., Xu, D., Tian, L., Chen, R., Wang, L., Tan, P., You, Q., 2019. Overwinter mortality in yellow drum (*Nibea albiflora*): insights from growth and immune responses to cold and starvation stress. Fish Shellfish Immunol. 92, 341–347. https://doi.org/10.1016/j.fsi.2019.06.030.

Su, Z.-L., Su, C.-W., Huang, Y.-L., Yang, W.-Y., Sampurna, B.P., Ouchi, T., Lee, K.-L., Wu, C.-S., Wang, H.-D., Yuh, C.-H., 2019. A novel AURKA mutant-induced early-onset severe hepatocarcinogenesis greater than wild-type via activating different pathways in zebrafish. Cancers 11, 927. https://doi.org/10.3390/cancers11070927.

Sun, Z., Tan, X., Liu, Q., Ye, H., Zou, C., Xu, M., Zhang, Y., Ye, C., 2019a. Physiological, immune responses and liver lipid metabolism of orange-spotted grouper (*Epinephelus coioides*) under cold stress. Aquaculture 498, 545–555. https://doi.org/10.1016/j.aquaculture.2018.08.051.

Sun, Z., Tan, X., Xu, M., Liu, Q., Ye, H., Zou, C., Ye, C., 2019b. Liver transcriptome analysis and de novo annotation of the orange-spotted groupers (*Epinephelus coioides*) under cold stress. Comp. Biochem. Physiol. D: Genom. Proteom. 29, 264–273. https://doi.org/10.1016/j.cbd.2018.12.008.

Todgham, A.E., Crombie, T.A., Hofmann, G.E., 2017. The effect of temperature adaptation on the ubiquitin–proteasome pathway in notothenioid fishes. J. Exp. Biol. 220, 369–378. https://doi.org/10.1242/jeb.145946.

Trapnell, C., Williams, B.A., Pertea, G., Mortazavi, A., Kwan, G., Van Baren, M.J., Salzberg, S.L., Wold, B.J., Pachter, L., 2010. Transcript assembly and quantification by RNA-Seq reveals unannotated transcripts and isoform switching during cell differentiation. Nat. Biotechnol. 28, 511–515. https://doi.org/10.1038/nbt.1621.

Wang, Y., Chen, Z., Wei, M., Lin, Z., Shen, M., Zhu, F., Jia, C., Meng, Q., Xu, D., Du, S., Liu, Y., Chen, S., Zhang, C., Zhang, Zhiyong, Zhang, Zhiwei, 2023. Liver transcriptome analysis of the black porgy (*Acanthopagrus schlegelii*) under acute low-temperature stress. Life 13, 721. https://doi.org/10.3390/life13030721.

Wen, B., Jin, S.-R., Chen, Z.-Z., Gao, J.-Z., 2018. Physiological responses to cold stress in the gills of discus fish (Symphysodon aequifasciatus) revealed by conventional biochemical assays and GC-TOF-MS metabolomics. Sci. Total Environ. 640–641, 1372–1381. https://doi.org/10.1016/j.scitotenv.2018.05.401.

Wen, X., Hu, Y., Zhang, X., Wei, X., Wang, T., Yin, S., 2019. Integrated application of multi-omics provides insights into cold stress responses in pufferfish Takifugu fasciatus. BMC Genomics 20, 1–15. https://doi.org/10.1186/s12864-019-5915-7.

Wu, S.M., Liu, J.-H., Shu, L.-H., Chen, C.H., 2015. Anti-oxidative responses of zebrafish (*Danio rerio*) gill, liver and brain tissues upon acute cold shock. Comp. Biochem. Physiol. A Mol. Integr. Physiol. 187, 202–213. https://doi.org/10.1016/j.cbpa.2015.05.016.

Wu, Q., Wu, Z., Wang, Lijuan, Lu, Y., Bi, W., Zhou, D., Wang, Ling, Peng, Z., You, F., 2021. Comparative study on growth performance and morphological characteristics of the meio- and mito-gynogenesis olive flounder (*Paralichthys olivaceus*). Aquaculture 535, 736387. https://doi.org/10.1016/j.aquaculture.2021.736387.

Xiao, J., Zou, T.M., Chen, L., Liu, S.J., Xiao, J., Zhang, H., Long, Y., Yan, J.P., Zhao, R.R., Tao, M., Zhang, C., You, C.P., Liu, Y., 2011. Microsatellite analysis of different ploidy offspring of artificial gynogenesis in *Cyprinus carpio*. J. Fish Biol. 78, 150–165. https://doi.org/10.1111/j.1095-8649.2010.02848.x.

Xu, K., Duan, W., Xiao, J., Tao, M., Zhang, C., Liu, Y., Liu, S., 2015. Development and application of biological technologies in fish genetic breeding. Sci. China Life Sci. 58, 187–201. https://doi.org/10.1007/s11427-015-4798-3.

Xu, Z., Li, T., Li, E., Chen, K., Ding, Z., Qin, J.G., Chen, L., Ye, J., 2016. Comparative transcriptome analysis reveals molecular strategies of oriental river prawn *Macrobrachium nipponense* in response to acute and chronic nitrite stress. Fish Shellfish Immunol. 48, 254–265. https://doi.org/10.1016/j.fsi.2015.12.005.

Yang, Y., Yu, Hui, Li, H., Wang, A., Yu, Hai-yi, 2016. Effect of high temperature on immune response of grass carp (Ctenopharyngodon idellus) by transcriptome analysis. Fish Shellfish Immunol. 58, 89–95. https://doi.org/10.1016/j.fsi.2016.09.014.

Yu, F.D., Gu, D.E., Tong, Y.N., Li, G.J., Wei, H., Mu, X.D., Xu, M., Yang, Y.X., Luo, D., Li, F.Y., Hu, Y.C., 2019. The current distribution of invasive mrigal carp (*Cirrhinus mrigala*) in southern China, and its potential impacts on native mud carp (*Cirrhinus*

molitorella) populations. J. Freshw. Ecol. 34, 603–616. https://doi.org/10.1080/02705060.2019.1655492.

Zhang, Z., Zhou, C., Fan, K., Zhang, L., Liu, Y., Liu, P., 2021. Metabolomics analysis of the effects of temperature on the growth and development of juvenile European seabass (*Dicentrarchus labrax*). Sci. Total Environ. 769, 145155 https://doi.org/10.1016/j.scitotenv.2021.145155.

Zhu, Y., Wu, Jinming, Leng, X., Du, H., Wu, Jinping, He, S., Luo, J., Liang, X., Liu, H., Wei, Q., Tan, Q., 2020. Metabolomics and gene expressions revealed the metabolic changes of lipid and amino acids and the related energetic mechanism in response to ovary development of Chinese sturgeon (*Acipenser sinensis*). PLoS One 15, e0235043. https://doi.org/10.1371/journal.pone.0235043.